

A peer-reviewed version of this preprint was published in PeerJ on 28 April 2015.

[View the peer-reviewed version](https://peerj.com/articles/918) (peerj.com/articles/918), which is the preferred citable publication unless you specifically need to cite this preprint.

Moore JK, Hnat SK, van den Bogert AJ. 2015. An elaborate data set on human gait and the effect of mechanical perturbations. PeerJ 3:e918
<https://doi.org/10.7717/peerj.918>

An elaborate data set on human gait and the effect of mechanical perturbations

Jason K. Moore¹, Sandra K. Hnat¹, and Antonie J. van den Bogert¹

¹Mechanical Engineering, Cleveland State University, Cleveland, Ohio, USA, 44115.
j.k.moore19@csuohio.edu, s.hnat@vikes.csuohio.edu, a.vandenbogert@csuohio.edu

ABSTRACT

Here we share a rich gait data set collected from fifteen subjects walking at three speeds on an instrumented treadmill. Each trial consists of 120 seconds of normal walking and 480 seconds of walking while being longitudinally perturbed during each stance phase with pseudo-random fluctuations in the speed of the treadmill belt. A total of approximately 1.5 hours of normal walking (> 5000 gait cycles) and 6 hours of perturbed walking (> 20,000 gait cycles) is included in the data set. We provide full body marker trajectories and ground reaction loads in addition to a presentation of processed data that includes gait events, 2D joint angles, angular rates, and joint torques along with the open source software used for the computations. The protocol is described in detail and supported with additional elaborate meta data for each trial. This data can likely be useful for validating or generating mathematical models that are capable of simulating normal periodic gait and non-periodic, perturbed gaits.

Keywords: gait, data, perturbation

INTRODUCTION

The collection of dynamical data during human walking has a long history beginning with the first motion pictures and now with modern marker based motion capture techniques and high fidelity ground reaction load measurements. Even though years of data on thousands of subjects now exist, this data is not widely disseminated, well organized, nor available with few or no restrictions. David Winter's published normative gait data (Winter, 1990) is widely used in biomechanical studies, yet it comes from few subjects and only a small number of gait cycles per subject. This small source has successfully enabled many other studies, such as powered prosthetic control design (Sup et al., 2008) but success in other research fields using large sets of data for discovery lead us to believe that more elaborate data sets may benefit the field of human motion studies. To enable such work, biomechanical data needs to be shared extensively, organized, and curated to enable future analysts.

There are some notable gait data sets and databases besides Winter's authoritative set that are publicly available. The International Society of Biomechanics has maintained a web page (<http://isbweb.org/data>) since approximately 1995 that includes data sets for download and mostly unencumbered use. For example, the kinematic and force plate measurements from several subjects from Vaughan et al. (1992) is available on the site. At another website, the CGA Normative Gait Database, Kirtley (2014) curates and shares normative clinical gait data collected from multiple labs and these datasets have influenced other studies, for example van den Bogert (2003) made use of the

27 average gait cycles from the child subjects.

28 Chester et al. (2007) report on a large gait database comparison where one database contained
29 kinematic data of 409 gait cycles of children from 1 to 7 years old but the data does not seem to
30 be publicly available. This is unfortunately typical. Tirosh et al. (2010) recognized the need for a
31 comprehensive data base for clinical gait data and created the Gaitabase. This database may contain
32 a substantial amount of data but it is encumbered by a complicated and restrictive license and sharing
33 scheme. Yun et al. (2014) provides lower body kinematic data of single gait cycles from over one
34 hundred subjects extracted from the large KIST Human Gait Pattern Data database which may also
35 include a substantial amount of raw data but it is private. However, there are examples of data with
36 less restrictions. The University of Wisconsin at LaCrosse has an easily accessible normative gait
37 data set (Willson and Kernozek, 2014) from 25 subjects with lower extremity marker data from
38 multiple gait cycles and force plate measurements from a single gait cycle. The CMU Graphics Lab
39 Motion Capture Database (Hodgins, 2015) is also a good example and contains full body marker
40 kinematics for a fair number of trials with small number of gait cycles during both walking and
41 running.

42 More recent examples of biomechanists sharing their data alongside publications are: van den
43 Bogert et al. (2013) which includes full body joint kinematics and kinetics from eleven subjects
44 walking on an instrumented treadmill and Wang and Srinivasan (2014) who include a larger set of
45 data from ten subjects walking for five minutes each at three different speeds but only a small set of
46 lower extremity markers are present. The second is notable because they publish the data in Dryad, a
47 modern citable data repository. It is also worth noting purely visual data collections of gait, like the
48 one presented in Makihara et al. (2012), which contain videos of subjects walking on a treadmill in
49 full clothing. This database is also unfortunately tightly secured with an extensive release agreement
50 for reuse.

51 The amount of publicly available gait data is small compared to the number of gait studies that
52 have been performed over the years. The data that is available generally suffers from limitations
53 such as few subjects, few gait cycles, few markers, highly clinical, no raw data, limited force plate
54 measurements, lack of meta data, non-standard formats, and restrictive licensing. To help with this
55 situation we are making the data we collected for our research purposes publicly available and free
56 of the previously mentioned deficiencies. Not only do we provide a larger set of normative gait data
57 that has been previously available, we also include an even larger set of data in which the subject
58 is being perturbed, something that does not currently exist. We believe both of these sets of data
59 can serve a variety of use cases and hope that we can save time and effort for future researchers by
60 sharing it.

61 But our reasons are not entirely altruistic, as governments and granting agencies are also
62 encouraging researchers to share data with recent policy changes. For example, the European
63 Commission (2012) has outlined publicly funded data's role in innovation and the White House
64 (2013) laid out a plan for public access to publications and data in 2013. The National Science
65 Foundation, which partially funds this work, was ahead of the White House and required all grants to
66 include a data management plan in 2011. This work is a partial fulfillment of the grant requirements
67 laid out in our grant's data management plan and we hope that this work can be a good model for
68 dissemination of biomechanical data.

69 Our use case for the data is centered around the need for bio-inspired control systems in emerging
70 powered prosthetics and orthotics. Ideally, a powered prosthetic would behave in such a way that
71 the user would feel like their limb was never disabled. There are a variety of approaches to

72 developing bio-inspired control systems, some of which aim to mimic the reactions and motion
73 of an able-bodied person. A modern gait lab is able to collect a variety of kinematic, kinetic, and
74 physiological data from humans during gait. This data can potentially be used to drive the design of
75 the human-mimicking controller. With a rich enough data set, one may be able to identify control
76 mechanisms used during a human's natural gait and recovery from perturbations. We hypothesize
77 that by forcing the human to recover from external perturbations, the resulting reactive actions can
78 be used along with system identification techniques to expose the feedback related relationships
79 among the human's sensors and actuators. With this in mind, we have collected data that is richer
80 than previous gait data sets and may be rich enough for control identification. The data can also
81 be used for verification purposes for controllers that have been designed in other manners, such as
82 those constructed from first principles, e.g. (Geyer and Herr, 2010).

83 With all of this in mind, we collected over seven and a half hours of gait data from fifteen able
84 bodied subjects which amounts to over 25,000 gait cycles (Moore et al., 2014a). The subjects walked
85 at three different speeds on an instrumented treadmill while we collected full body marker locations
86 and ground reaction loads from a pair of force plates. The final protocol for the majority of the
87 trials included two minutes of normal walking and eight minutes of walking under the influence of
88 pseudo-random belt speed fluctuations. The data has been organized complete with rich meta data
89 and made available in the most unrestrictive form for other research uses following modern best
90 practices in data sharing (White et al., 2013).

91 Furthermore, we include a small Apache licensed open source software library for basic gait
92 analysis and demonstrate its use in the paper. The combination of the open data and open software
93 allow the results presented within to be computationally reproducible and instructions are included
94 in the associated repository ¹ for reproducing the results.

95 METHODS

96 In this section, we describe our experimental design beginning with descriptions of the participants
97 and equipment. This is then followed by the protocol details and specifics on the perturbation design.

98 Participants

99 Fifteen able bodied subjects including four females and eleven males with an average age of 24 ± 4
100 years, height of 1.75 ± 0.09 m, mass of 74 ± 13 kg participated in the study. The study was approved
101 by the Institutional Review Board of Cleveland State University (# 29904-VAN-HS) and written
102 informed consent was obtained from all participants. The data has been anonymized with respect
103 to the participants' identities and a unique identification number was assigned to each subject. A
104 selection of the meta data collected for each subject is shown in Table 1.

105 Equipment

106 The data were collected in the Laboratory for Human Motion and Control at Cleveland State
107 University, using the following equipment:

- 108 • A R-Mill treadmill which has dual 6 degree of freedom force plates, independent belts for
109 each foot, along with lateral translation and pitch rotation capabilities (Forcelink, Culemborg,
110 Netherlands).

¹<https://github.com/csu-hmc/perturbed-data-paper>

Table 1. Information about the 15 study participants in order of collection date. The subjects are divided into those that were used for the protocol pilot trials, i.e. the first three, and those used for the final protocol. The final three columns provide the trial numbers associated with each nominal treadmill speed. The measured mass is computed from the mean total vertical ground reaction force just after the calibration pose event, if possible. If the mass is reported without an accompanying standard deviation, it is the subject's self-reported mass. Additional trials found in the data set with a subject identification number 0 are trials with no subject, i.e. unloaded trials that can be used for inertial compensation purposes, and are not shown in the table. Generated by `src/subject_table.py`.

| Id | Gender | Age [yr] | Height [m] | Mass [kg] | 0.8 m/s | 1.2 m/s | 1.6 m/s |
|----|--------|----------|------------|----------------|---------|---------|---------|
| 1 | male | 25 | 1.87 | 101 | NA | 6, 7, 8 | NA |
| 11 | male | 22 | 1.85 | 80 | 9 | 10 | 11 |
| 4 | male | 30 | 1.76 | 74 | 12, 15 | 13 | 14 |
| 7 | female | 29 | 1.72 | 64.5 ± 0.8 | 16 | 17 | 18 |
| 8 | male | 20 | 1.57 | 74.9 ± 0.9 | 19 | 20 | 21 |
| 9 | male | 20 | 1.69 | 67 ± 2 | 25 | 26 | 27 |
| 5 | male | 23 | 1.73 | 71.2 ± 0.9 | 32 | 31 | 33 |
| 6 | male | 26 | 1.77 | 86.8 ± 0.6 | 40 | 41 | 42 |
| 3 | female | 32 | 1.62 | 54 ± 2 | 46 | 47 | 48 |
| 12 | male | 22 | 1.85 | 74.2 ± 0.5 | 49 | 50 | 51 |
| 13 | female | 21 | 1.70 | 58 ± 2 | 55 | 56 | 57 |
| 10 | male | 19 | 1.77 | 92 ± 2 | 61 | 62 | 63 |
| 15 | male | 22 | 1.83 | 80.5 ± 0.8 | 67 | 68 | 69 |
| 17 | male | 23 | 1.86 | 88.3 ± 0.8 | 73 | 74 | 75 |
| 16 | female | 28 | 1.69 | 56.2 ± 0.6 | 76 | 77 | 78 |

- 111 • A 10 Osprey camera motion capture system paired with the Cortex 3.1.1.1290 software
112 (Motion Analysis, Santa Rosa, CA, USA).
- 113 • USB-6255 data acquisition unit (National Instruments, Austin, Texas, USA).
- 114 • Four ADXL330 Triple Axis Accelerometer Breakout boards attached to the treadmill (Spark-
115 fun, Niwot, Colorado, USA).
- 116 • D-Flow software (versions 3.16.1 to 3.16.2) and visual display system, (Motek Medical,
117 Amsterdam, Netherlands).

118 The Cortex software delivers high accuracy 3D marker trajectories from the cameras along
119 with data from the force plates and analog sensors (e.g. EMG/Accelerometer) through a National
120 Instruments USB-6255 data acquisition unit. D-Flow then receives streaming data from Cortex and
121 any other digital sensors. It is also responsible for controlling the treadmill's motion (lateral, pitch,
122 belts). D-Flow can process the data in real time and/or export data to file.

123 Our motion capture system's coordinate system is such that the X coordinate points to the right,
124 the Y coordinate points upwards, and the Z coordinate follows from the right-hand-rule, i.e. points
125 backwards with respect to the walking direction. The camera's coordinate system is aligned to an
126 origin point on the treadmill's surface during camera calibration. The same point is used as the
127 origin of the ground reaction force measuring system. Figure 1 shows the layout of the equipment.

128 Early on, we discovered that the factory setup of the R-Link treadmill had a vibration mode as
129 low as 5Hz that was detectable in the force measurements; likely due to the flexible undercarriage
130 and pitch motion mechanism. Trials 6–8 are affected by this vibration mode. During trials 9–15
131 the treadmill was stabilized with wooden blocks. During the remaining trials (> 15) the treadmill
132 was stabilized with metal supports; both with ones we fabricated in-house and ones supplied by the
133 vendor. These supports aimed to improve the stiffness and frequency response of the force plate
134 system. See the Data Limitations Section for more details.

135 The acceleration of the treadmill base was measured during each trial by the ADXL330 ac-
136 celerometers placed at the four corners of the machine. These accelerometers were intended to
137 provide information for inertial compensation purposes when the treadmill moved laterally or in
138 pitch, but are extraneous for trials greater than number 8 due to the treadmill being stabilized in
139 those degrees of freedom by the aforementioned supports.

140 Protocol

141 The experimental protocol consisted of both static measurements and walking on the treadmill for
142 10 minutes under unperturbed and perturbed conditions. Before a set of trials on the same day, the
143 motion capture system was calibrated using the manufacturer's recommended procedure. Before
144 each subject's gait data were collected, the subject changed into athletic shoes, shorts, a sports bra, a
145 baseball cap², and a rock climbing harness. All 47 markers were applied directly to the skin at the
146 landmarks noted in Table 2 except for the heel, toe, and head markers, which were placed on the
147 respective article of clothing.³ Then the subject self-reported their age, gender, and mass. Finally,
148 their height was measured by the experimentalist and four reference photographs (front, back, right,
149 left) were taken of subject's marker locations.

²A cap was used to avoid having to shave participants' hair at the expense of accuracy.

³The sacrum and rear pelvic markers were placed on the shorts for a small number of the subjects.

Table 2. Descriptions of the 47 subject markers used in this study. The “Set” column indicates whether the marker exists in the lower and/or full body marker set. The label column matches the column headers in the mocap-xxx.txt files and/or the marker map in the meta-xxx.yml file.

| Set | # | Label | Name | Description |
|-----|----|-------|---------------------------------------|---|
| F | 1 | LHEAD | Left head | Just above the ear, in the middle. |
| F | 2 | THEAD | Top head | On top of the head, in line with the LHEAD and RHEAD. |
| F | 3 | RHEAD | Right head | Just above the ear, in the middle. |
| F | 4 | FHEAD | Forehead | Between line LHEAD/RHEAD and THEAD a bit right from center. |
| L/F | 5 | C7 | C7 | On the 7th cervical vertebrae. |
| L/F | 6 | T10 | T10 | On the 10th thoracic vertebrae. |
| L/F | 7 | SACR | Sacrum bone | On the sacral bone. |
| L/F | 8 | NAVE | Navel | On the navel. |
| L/F | 9 | XYPH | Xiphoid process | Xiphoid process of the sternum. |
| F | 10 | STRN | Sternum | On the jugular notch of the sternum. |
| F | 11 | BBAC | Scapula | On the inferior angle fo the right scapular. |
| F | 12 | LSHO | Left shoulder | Left acromion. |
| F | 13 | LDEL | Left deltoid muscle | Apex of the deltoid muscle. |
| F | 14 | LLEE | Left lateral elbow | Left lateral epicondyle of the elbow. |
| F | 15 | LMEE | Left medial elbow | Left medial epicondyle of the elbow. |
| F | 16 | LFRM | Left forearm | On 2/3 on the line between the LLEE and LMW. |
| F | 17 | LMW | Left medial wrist | On styloid process radius, thumb side. |
| F | 18 | LLW | Left lateral wrist | On styloid process ulna, pinky side. |
| F | 19 | LFIN | Left fingers | Center of the hand. Caput metatarsal 3. |
| F | 20 | RSHO | Right shoulder | Right acromion. |
| F | 21 | RDEL | Right deltoid muscle | Apex of deltoid muscle. |
| F | 22 | RLEE | Right lateral elbow | Right lateral epicondyle of the elbow. |
| F | 23 | RMEE | Right medial elbow | Right medial epicondyle of the elbow. |
| F | 24 | RFRM | Right forearm | On 1/3 on the line between the RLEE and RMW. |
| F | 25 | RMW | Right medial wrist | On styloid process radius, thumb side. |
| F | 26 | RLW | Right lateral wrist | On styloid process ulna, pinky side. |
| F | 27 | RFIN | Right fingers | Center of the hand. Caput metatarsal 3. |
| L/F | 28 | LASIS | Pelvic bone left front | Left anterior superior iliac spine. |
| L/F | 29 | RASIS | Pelvic bone right front | Right anterior superior iliac spine. |
| L/F | 30 | LPSIS | Pelvic bone left back | Left posterior superio iliac spine. |
| L/F | 31 | RPSIS | Pelvic bone right back | Right posterior superior iliac spine. |
| L/F | 32 | LGTRO | Left greater trochanter of the femur | On the cetner of the left greater trochanter. |
| L/F | 33 | FLTHI | Left thigh | On 1/3 on the line between the LFTRO and LLEK. |
| L/F | 34 | LLEK | Left lateral epicondyle of the knee | On the lateral side of the joint axis. |
| L/F | 35 | LATI | Left anterior of the tibia | On 2/3 on the line between the LLEK and LLM. |
| L/F | 36 | LLM | Left lateral malleolus of the ankle | The center of the heel at the same height as the toe. |
| L/F | 37 | LHEE | Left heel | Center of the heel at the same height as the toe. |
| L/F | 38 | LTOE | Left toe | Tip of big toe. |
| L/F | 39 | LMT5 | Left 5th metatarsal | Caput of the 5th metatarsal bone, on joint line midfoot/toes. |
| L/F | 40 | RGTRO | Right greater trochanter of the femur | On the cetner of the right greater trochanter. |
| L/F | 41 | FRTHI | Right thigh | On 2/3 on the line between the RFTRO and RLEK. |
| L/F | 42 | RLEK | Right lateral epicondyle of the knee | On the lateral side of the joint axis. |
| L/F | 43 | RATI | Right anterior of the tibia | On 1/3 on the line between the RLEK and RLM. |
| L/F | 44 | RLM | Right lateral malleolus of the ankle | The center of the heel at the same height as the toe. |
| L/F | 45 | RHEE | Right heel | Center of the heel at the same height as the toe. |
| L/F | 46 | RTOE | Right toe | Tip of big toe. |
| L/F | 47 | RMT5 | Right 5th metatarsal | Caput of the 5th metatarsal bone, on joint line midfoot/toes. |



Figure 1. The treadmill with coordinate system, cameras (circled in orange), projection screen, and safety rope. The direction of travel is in the $-z$ direction.

After obtaining informed consent and a briefing by the experimentalist on the trial protocol, the subject followed the verbal instructions of the experimentalist and the on-screen instructions from the video display. The final protocol for a single trial was as follows:

1. The subject stepped onto the treadmill and markers were identified with Cortex.
2. The safety rope was attached loosely to the rock climbing harness such that no forces were acting on the subject during walking, but so that the harness would prevent a full fall.
3. The subject started by stepping on sides of treadmill so that feet did not touch the force plates and the force plate signals are zeroed. This corresponds to the “Force Plate Zeroing” event.
4. Once notified by the video display, the subject stood in the calibration pose: standing straight up, looking forward, arms out by their sides (approximately 45 degree abduction) and the event, “Calibration Pose”, was manually recorded by the operator.
5. A countdown to the first normal walking phase was displayed. At the end of the countdown the event “First Normal Walking” was recorded and the treadmill ramped up to the specified speed and the subject was instructed to walk normally, to focus on the “endless” road on the display, and not to look at their feet.
6. After 1 minute of normal walking, the longitudinal perturbation phase begun and was recorded as “Longitudinal Perturbation”.
7. After 8 minutes of walking under the influence of the perturbations, the second normal walking phase begun and was recorded as “Second Normal Walking”.
8. After 1 minute of normal walking, a countdown was shown on the display and the treadmill decelerated to a stop.

171 9. The subject was instructed to step off of the force plates for 10 seconds and the “Unloaded
172 End” event was recorded.

173 10. The subject could then take a rest break before each additional trial.

174 ***Pilot Protocols***

175 Trials 3–15 were pilot tests for finalizing the protocol design and thus have some slight variations
176 with respect to the subsequent trials. We include these trials due to the uniqueness of trials 6–8 and
177 the fact that the kinematic data is valid. We believe there may be useful analyses that only require
178 the kinematic data. Additional information needed to interpret the data in the pilot trials can be
179 found in the associated meta data files and the Data Limitations Section of this paper.

180 Trials 3–8 use an early experimental protocol which divided the walking period into three
181 sections: no perturbation, longitudinal perturbation, and a combination of longitudinal and lateral
182 perturbation. The calibration pose and zeroing events are present in the data but lumped into one
183 event. These trials only use the lower body marker set described in Table 2. Additionally, there are
184 five markers that have labels beginning with ROT that were attached to the treadmill base to capture
185 the lateral motion. Trials 9–15 use the final protocol but have corrupt ground reaction loads due to
186 the wooden treadmill base stabilizers.

187 **Perturbation Signals**

188 As previously described, the protocol included a phase of normal walking, followed by longitudinal
189 belt speed perturbations, and ended with a second segment of normal walking. Three pseudo-random
190 belt speed control signals, with mean velocities of 0.8 m s^{-1} , 1.2 m s^{-1} and 1.6 m s^{-1} , were pre-
191 generated with MATLAB and Simulink (Mathworks, Natick, Massachusetts, USA) and are available
192 for download from Zenodo (Hnat et al., 2015). The same control signal was used for all trials at that
193 given speed.

194 To create the signals, we started by generating random acceleration signals, sampled at 100 Hz,
195 using the Simulink discrete-time Gaussian white noise block followed by a saturation block set at the
196 maximum belt acceleration of 15 m s^{-2} . The signal was then integrated to obtain belt speed and high-
197 pass filtered with a second-order Butterworth filter to eliminate drift. One of the three mean speeds
198 were then added to the signal and limited between 0 m s^{-1} to 3.6 m s^{-1} . The cutoff frequencies
199 of the high-pass filter, as well as the variance in the acceleration signal, were manually adjusted
200 until acceptable standard deviations for each mean speed were obtained: 0.06 m s^{-1} , 0.12 m s^{-1} and
201 0.21 m s^{-1} for the three speeds, respectively. These ensured that the test subjects were sufficiently
202 perturbed at each speed, while remaining within the limits of our equipment and testing protocol.
203 To ensure that the treadmill belts could accelerate to the desired values, the high performance
204 mode in the D-Flow software was enabled. The MATLAB script and Simulink model produce a
205 comma-delimited text file of with the desired belt speed signals indexed by the time stamp.

206 Figure 2 gives an idea of the effect of the treadmill and controller dynamics by plotting the
207 measured speed of the treadmill belts from loaded trials (76, 77, 78) against the commanded treadmill
208 control input signal. The system introduces a delay and seems to act as a low pass filter. The standard
209 deviations of the measured speeds do not significantly differ from those of the commanded speeds:
210 0.05 m s^{-1} , 0.12 m s^{-1} and 0.2 m s^{-1} for the three speeds, respectively.

211 Figure 3 gives a frequency domain view of the effects of the treadmill dynamics. These spectral
212 density plots were created by averaging a spectrogram of a twenty second Hamming window. For

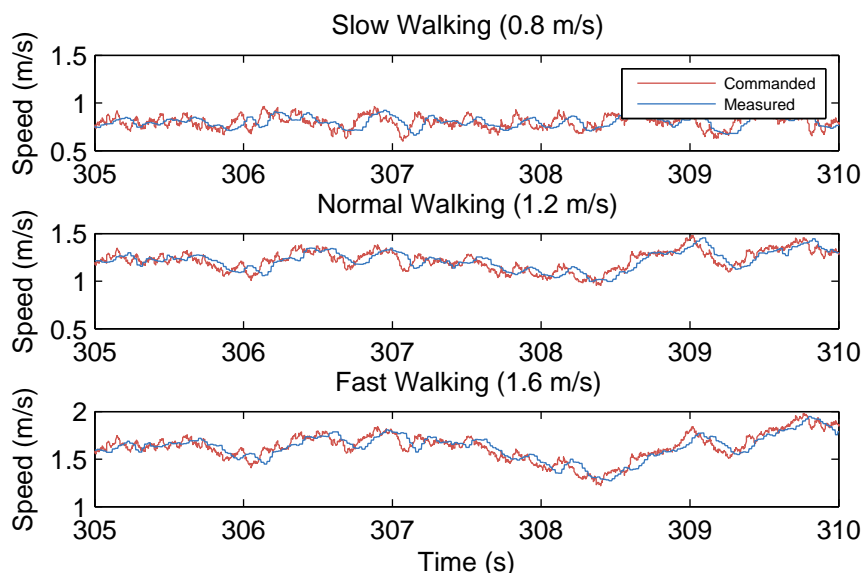


Figure 2. Commanded treadmill belt speed (red) and the recorded speed (blue) for average belt speeds of 0.8 m s^{-1} , 1.2 m s^{-1} and 1.6 m s^{-1} , respectively. Generated by `src/input_output_plot.m`.

Table 3. A list of unloaded trials collected for each speed. Each loaded trial includes a compensation file listed in its meta data which matches it to these unloaded trials. Generated by `src/subject_table.py`.

| Speed | Trial Numbers |
|---------|---|
| 0.8 m/s | 22, 30, 34, 43, 52, 58, 64, 70, 79 |
| 1.2 m/s | 3, 4, 5, 23, 29, 35, 44, 53, 59, 65, 71, 80 |
| 1.6 m/s | 24, 28, 36, 45, 54, 60, 66, 72, 81 |

213 all speeds, the frequency content of the commanded and measured time series show similarity below
214 4 Hz and attenuation in the measured spectral density above 4 Hz.

215 When belt speed is not constant, the inertia of the rollers and motor will likely induce error in
216 the force plate x axis moment, and hence, the anterior-posterior coordinate (z axis) of the center
217 of pressure that is measured by the instrumentation in the treadmill. This error may or may not be
218 pertinent to different analyses. If needed, this error can be partially compensated by a linear model
219 as shown in Hnat and van den Bogert (2014). The model coefficients can be identified from the
220 unloaded trials given in Table 3. The error due to inertia is random and does not affect the averaged
221 joint moments presented in Figure 5. Compensation should, however, be done if joint moments from
222 individual gait cycles are of interest rather than the ensemble average.

223 In addition to the longitudinal perturbations, lateral perturbations were also prescribed for a
224 duration of four minutes in the pilot trials 3–8. Figure 4 shows an example of the measured lateral
225 deviation of the treadmill base. These signals were generated in a similar manner using MATLAB
226 and Simulink in which a Gaussian white noise block was twice integrated to obtain the lateral
227 deviation. The signal was then high-pass filtered with a second-order Butterworth filter to eliminate

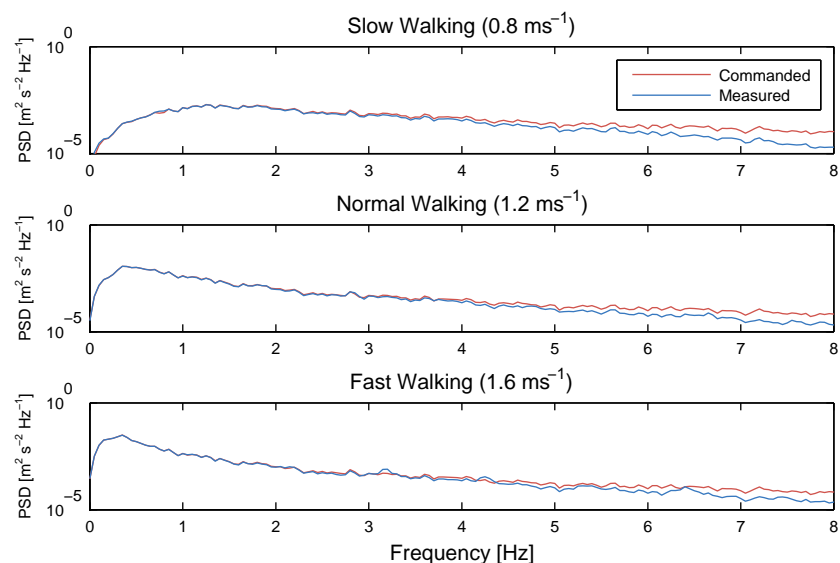


Figure 3. Power spectral density of the commanded treadmill belt speed (red) and the recorded speed (blue) for average belt speeds of 0.8 m s^{-1} , 1.2 m s^{-1} and 1.6 m s^{-1} , respectively. Generated by `src/frequency_analysis.m`.

228 drift and then saturated so that the signal remained within the 5 cm lateral range of the physical
 229 hardware. The same perturbation signal was used for each of the three trials.

230 RESULTS

231 Here we present some basic results. We first provide a detailed description of the raw data followed
 232 by an overview of several computed variables that give an idea of the characteristics of both the
 233 unperturbed and perturbed gait.

234 Raw Data

235 The raw data consists of a set of ASCII tab delimited text files output from both the “mocap” and
 236 “record” modules in D-Flow in addition to a manually generated YAML⁴ file that contains all of the
 237 necessary meta data for the given trial. These three files are stored in a hierarchy of directories with
 238 one trial per directory. The directories are named in the following fashion `T001/` where T stands
 239 for “trial” and the following three digits provide a unique trial identification number.

240 *mocap-xxx.txt*

241 The output from the D-Flow mocap module is stored in a tab separated value (TSV) file named
 242 `mocap-xxx.txt` where `xxx` represents the trial id number. The file contains a number of time
 243 series. The numerical values of the time series are provided in decimal fixed point notation with
 244 6 decimals of precision, e.g. `123456.123456`, regardless of the units. The first line of the file
 245 holds the header. The header includes time stamp column, frame number column, marker position
 246 columns, force plate force/moment columns, force plate center of pressure columns, and other
 247 analog columns. The columns are further described below:

⁴YAML is a human readable data serialization format. See Listing 1 for an example.

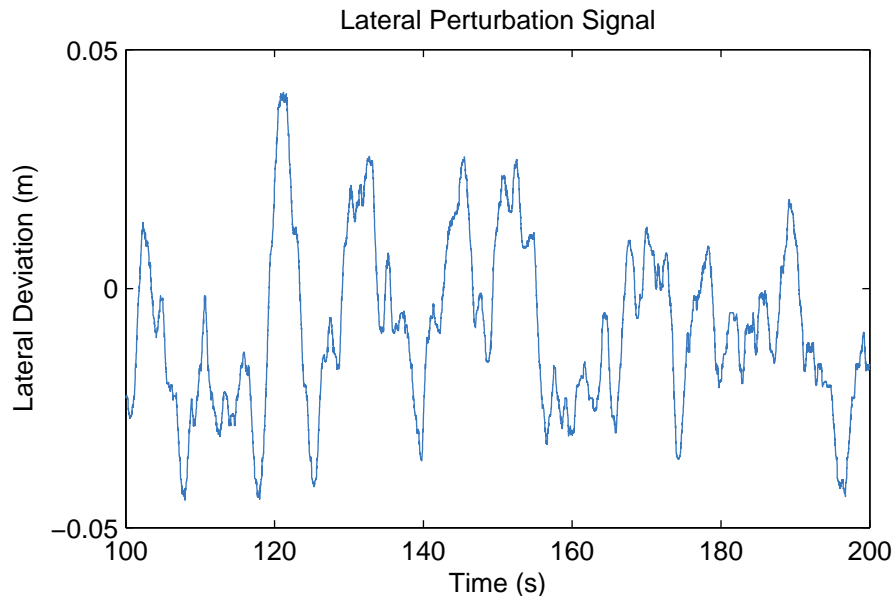


Figure 4. The measured lateral deviation of the treadmill base from trial 6. Generated by `src/lateral_perturbation_plot.m`.

248 **TimeStamp** The monotonically increasing computer clock time when D-Flow receives a frame
 249 from Cortex. These are recorded approximately at 100 Hz sampling rate and given in seconds.
 250 Due to data buffering, it is preferred to derive sample times from the FrameNumber column
 251 rather than the TimeStamp.

252 **FrameNumber** Monotonically increasing positive integers that correspond to each frame received
 253 from Cortex.

254 **Marker Coordinates** Any column that ends in `.PosX`, `.PosY`, or `.PosZ` are marker coordinates
 255 expressed in Cortex's Cartesian reference frame. The prefixes match the marker labels given
 256 in Table 2. These values are in meters.

257 **Ground Reaction Loads** There are three ground reaction forces and three ground reaction moments
 258 recorded by each of the two force plates in Newtons and Newton-Meters, respectively. The
 259 prefix for these columns is either `FP1` or `FP2` and represents either force plate 1 (left) or
 260 2 (right). The suffixes are either `.For[XYZ]`, `.Mom[XYZ]` for the forces and moments,
 261 respectively. The force plate voltages are sampled at a much higher frequency than the
 262 cameras, but delivered at the Cortex camera sample rate, approximately 100 Hz, through the
 263 D-Flow mocap module. A force/moment calibration matrix stored in Cortex converts the
 264 voltages to forces and moments before sending it to D-Flow. The software also computes the
 265 center of pressure from the forces, moments, and force plate dimensions. These have the same
 266 prefixes for the plate number, have the suffix `.Cop[XYZ]`, and are given in meters.

267 **Analog Channels** Several analog signals are recorded under column headers `Channel[1-99].Anlg`.
 268 These correspond to analog signals sampled by Cortex and correspond to the 96 analog chan-
 269 nels in the National Instruments USB-6255. The first twelve are the voltages from the force
 270 plate load cells. We also record the acceleration of 4 points on the treadmill base in analog

271 channels 61–72 that were in place in case inertial compensation for the lateral treadmill
272 movement was required.

273 We make use of the full body 47 marker set described in van den Bogert et al. (2013) and
274 presented in detail in Table 2. As with all camera based motion capture systems, the markers
275 sometimes go missing in the recording. When a marker goes missing, if the data was recorded in a
276 D-Flow version less than 3.16.2rc4, D-Flow continues to record the last non-missing value in all
277 three axes until the marker is visible again. In D-Flow versions greater than or equal to 3.16.2rc4, the
278 missing markers are indicated in the TSV file as either 0.000000 or -0.000000. The D-Flow
279 version must be provided in the meta data YAML file to be able to distinguish this detail.

280 *record-xxx.txt*

281 The record module also outputs a tab delimited ASCII text file with numerical values at six decimal
282 digits. It includes a `Time` column which records the D-Flow system time in seconds. This time
283 corresponds to the time recorded in the `TimeStamp` column in mocap module TSV file which is
284 necessary for time synchronization. There are two additional columns `RightBeltSpeed` and
285 `LeftBeltSpeed` which provide the independent belt speeds measured in meters per second by a
286 factory installed encoder in the treadmill.

287 Additionally, the record module is capable of recording the time at which various preprogrammed
288 events occur, as detected or set by D-Flow. It does this by inserting commented (#) lines in between
289 the rows when the event occurred. The record files have several events that delineate the different
290 phases of the protocol:

291 **A: Force Plate Zeroing** Marks the time at the beginning of the trial at which there is no load on
292 the force plates and when the force plate voltages were zeroed.

293 **B: Calibration Pose** Marks the time at which the person is in the calibration pose.

294 **C: First Normal Walking** Marks the time when the treadmill begins Phase 1: constant belt speed.

295 **D: Longitudinal Perturbation** Marks the time when the treadmill begins Phase 2: longitudinal
296 perturbations in the belt speed.

297 **E: Second Normal Walking** Marks the time when phase 3 starts: constant belt speed.

298 **F: Unloaded End** Marks the time at which there is no load on the force plates and the belts are
299 stationary.

300 *meta-xxx.yml*

301 Each trial directory contains a meta data file in the YAML format named in the following style
302 `meta-xxx.yml` where `xxx` is the three digit trial identification number. There are three main
303 headings in the file: `study`, `subject`, and `trial`. An example meta data file is shown in
304 Listing 1.

305 The `study` section contains identifying information for the overall study, an identification
306 number, name, and description. This is the same for all meta data files in the study. Details are given
307 below:

308 **id** An integer specifying a unique identification number of the study.

309 **name** A string giving the name of the study.

310 **description** A string with a basic description of the study.

311 The `subject` section provides key value pairs of information about the subject in that trial.
312 Each subject has a unique identification number along with basic anthropomorphic data. The
313 following details the possible meta data for the subject:

314 **age** An integer age in years of the subject at the time of the trial.

315 **ankle-width-left** A float specifying the width of the subjects left ankle.

316 **ankle-width-right** A float specifying the width of the subjects right ankle.

317 **ankle-width-units** A string giving the units of measurement of the ankle widths.

318 **id** An unique identification integer for the subject.

319 **gender** A string specifying the gender of the subject.

320 **height** A float specifying the measured height of the subject (with shoes and hat on) at the time of
321 the trial.

322 **height-units** A string giving the units of the height measurement.

323 **knee-width-left** A float specifying the width of the subjects left knee.

324 **knee-width-right** A float specifying the width of the subjects right knee.

325 **knee-width-units** A string giving the units of measurement of the knee widths.

326 **mass** A float specifying the self-reported mass of the subject.

327 **mass-units** A string specifying the units of the mass measurement.

328 The `trial` section contains the information about the particular trial. Each trial has a unique
329 identification number along with a variety of other information, detailed below:

330 **analog-channel-map** A mapping of the strings D-Flow assigns to signals emitted from the analog
331 channels of the NI USB-6255 to names the user desires.

332 **cortex-version** The version of Cortex used to record the trial.

333 **datetime** A date formatted string giving the date of the trial in the YYYY-MM-DD format.

334 **dflow-version** The version of D-Flow used to record the trial.

335 **events** A key value map which prescribes names to the alphabetic events recorded in the record file.

336 **files** A key value mapping of files associated with this trial where the key is the D-Flow file type
337 and the value is the path to the file relative to the meta file. The compensation file corresponds
338 to an unloaded trial collected on the same day that could be used for inertial compensation
339 purposes, if needed.

340 **hardware-settings** There are tons of settings for the hardware in both D-Flow, Cortex, and the
341 other software in the system. This contains any non-default settings.

342 **high-performance** A boolean value indicating whether the D-Flow high performance setting
343 was on (True) or off (False).

344 **id** An unique three digit integer identifier for the trial. All of the file names and directories associated
345 with this trial include this number.

346 **marker-map** A key value map which maps marker names in the mocap file to the user's desired
347 names for the markers.

348 **marker-set** Indicates the HBM (van den Bogert et al., 2013) marker set used during the trial, either
349 full, lower, or NA.

350 **nominal-speed** A float representing the nominal desired treadmill speed during the trial.

351 **nominal-speed-units** A string providing the units of the nominal speed.

352 **notes** A string with any notes about the trial.

353 **pitch** A boolean that indicates if the treadmill pitch degree of freedom was actuated during the trial.

354 **stationary-platform** A boolean that indicates whether the treadmill sway or pitch motion was
355 actuated during the trial. If this flag is false, the measured ground reaction loads must be
356 compensated for the inertial affects and be expressed in the motion capture reference frame.

357 **subject-id** An integer corresponding to the subject in the trial.

358 **sway** A boolean that indicates if the treadmill lateral degree of freedom was actuated during the
359 trial.

360 **Processed Data**

361 We developed a toolkit for data processing, GaitAnalysisToolKit v0.1.2 (Moore et al., 2014b) for
362 common gait computations and provide an example processed trial to present the nature of the
363 data. The tool was developed in Python, is dependent on the SciPy Stack [NumPy (Walt et al.,
364 2011), SciPy (Jones et al., 2001), matplotlib (Hunter, 2007), Pandas (McKinney, 2010), etc] and
365 Octave (Octave community, 2014), and provides two main classes: one to do basic gait data cleaning
366 from D-Flow's output files, `DFlowData`, and a second to compute common gait variables of
367 interest, `GaitData`.

368 The `DFlowData` class collects and stores all the raw data presented in the previous section and
369 applies several "cleaning" operations to transform the data into a usable form. The cleaning process
370 follows these steps:

371 1. Load the meta data file into a Python dictionary.

372 2. Load the D-Flow mocap module TSV file into Pandas `DataFrame`.

- PeerJ PrePrints
- 373 3. Relabel the column headers to more meaningful names if this is specified in the meta data.
 - 374 4. Optionally identify the missing values in the mocap marker data and replace them with
375 `numpy.nan`.
 - 376 5. Optionally interpolate the missing marker values and replaces them with interpolated estimates
377 using a variety of interpolation methods.
 - 378 6. Load the D-Flow record module TSV file into a `Pandas DataFrame`.
 - 379 7. Extract the events and create a dictionary mapping the event names in the meta data to the
380 events detected in the record module file.
 - 381 8. Inertially compensate the ground reaction loads based on whether the meta data indicates
382 there was treadmill motion.
 - 383 9. Merge the data from the mocap module and record module into one data frame at the maximum
384 common constant sample rate.

385 Once the data is cleaned there are two methods that allow the user to extract the cleaned data:
386 either extract sections of the data bounded by the events recorded in the `record-xxx.txt` file or
387 save the cleaned data to disk. These operations are available as a command line application and as
388 an application programming interface (API) in Python. An example of the `DFlowData` API in use
389 is provided in Listing 2.

390 The `GaitData` class is then used to compute gait events (toe off and heel strike times), basic
391 2D inverse kinematics and dynamics, and to store the data into a `Pandas Panel` with each gait cycle
392 on the item axis at a specified sampling rate. This object can also be serialized to disk in HDF5
393 format. An example of using the Python API is shown in Listing 3.

394 A similar work flow was used to produce Figure 5 which compares the mean and standard
395 deviation of sagittal plane joint angles and torques from the perturbed gait cycles to the unperturbed
396 gait cycles computed from trial 20. This gives an idea of the more highly variable dynamics required
397 to walk while being longitudinally perturbed.

398 For more insight into the difference in the unperturbed and perturbed data, Figure 6 compares
399 the distribution of a few gait cycle statistics. One can see that the perturbed strides have a much
400 larger variation in frequency and length and even larger variation in stride width. It is also interesting
401 to note that the coupled nature of the system's degrees of freedom can be exploited to increase the
402 stride width with only longitudinal perturbations, although not relatively as much as is in the other
403 statistics.

404 **Data Limitations**

405 The data is provided in good faith with great attention to detail but as with all data there are anomalies
406 that may affect the use and interpretation of results emanating from the data. The following lists
407 give various notes and warnings about the data that should be taken into account before use.

408 **All Trials**

- 409 • Be sure to read the notes in each meta data file for details about possible anomalies in that
410 particular trial. Things such as marker dropout, ghost markers, and marker movement are the

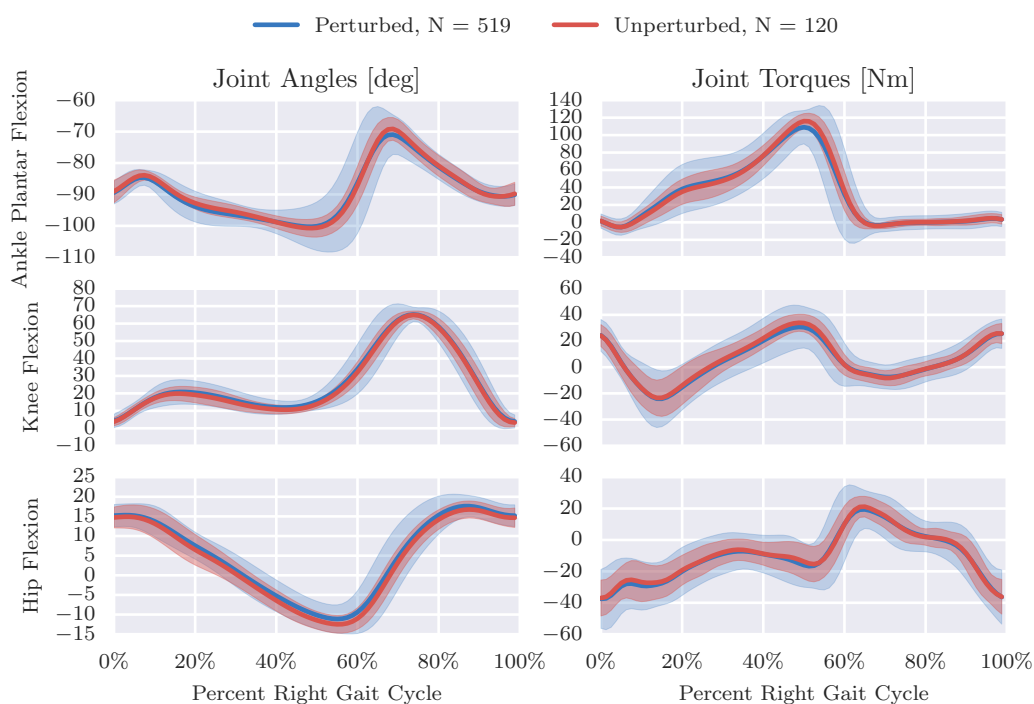


Figure 5. Right leg mean and 3σ (shaded) joint angles and torques from both unperturbed (red) and perturbed (blue) gait cycles from trial 20. We define the nominal configuration, i.e. all joint angles equal to zero, such that the vectors from the shoulder to the hip, the hip to the knee, the knee to the ankle, and the heel to the toe are all aligned. Produced by `src/unperturbed_perturbed_comparison.py`.

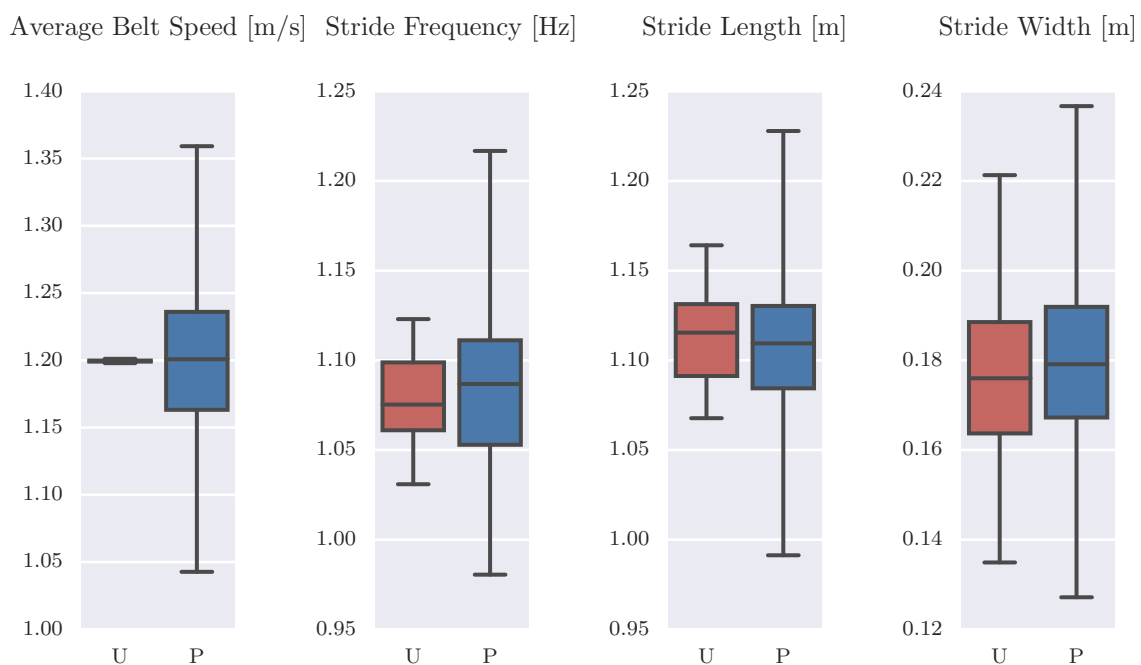


Figure 6. Box plots of the average belt speed, stride frequency, stride length, and stride width which compare 120 unperturbed (U: red) and 519 perturbed (P: blue) gait cycles. The median is given with the box bounding the first and third quartiles and the whiskers bound the range of the data. Produced by `src/unperturbed_perturbed_comparison.py`.

411 more prominent notes. Details about variations in the equipment on the day of the trial are
412 also mentioned.

413 ● The subject identification number 0 represents the “null subject” and was used whenever data
414 was collected from the system with no subject on the treadmill, for example during the trials
415 that were intended to be used for inertial compensation purposes. These trials play through
416 the exact protocol as those with a human subject and the matching trials are indicated in the
417 meta data. Matching unloaded trials were recorded on the same day as the loaded trials and is
418 noted in the `trial:files:compensation` section of the meta data file. See Table 3 for
419 a list of all the compensation trials.

420 ● Trials 1 and 2 were not recorded as part of this study. Those trial identification numbers were
421 reserved for early data exploration from data collected in other studies and are not included in
422 this dataset.

423 ● Trials 37, 38, and 39 do not exist. The numbers were accidentally skipped.

424 ● The ankle joint torques computed from subject 9’s data in trials 25–27 are abnormal and
425 should be used with caution or not at all. We were not able to locate the source of the error,
426 but it is likely related to the force calibration.

427 ***Pilot Trials***

428 ● Subject 1 walked only at a single speed with three trial repetitions.

429 ● Trials 6–8 included a calibration pose at the start of the trial but the event was not explicitly
430 recorded. In those trials, the “TreadmillPerturbation” event marks the beginning of longitudinal
431 perturbations and the “Both” event marks the beginning of combined longitudinal and lateral
432 perturbations. The force plate zeroing at the end was also not explicitly recorded.

433 ● Trials 6–8’s force measurements are affected by the treadmill vibration mode mentioned in
434 the equipment section and the force plate data should not be used.

435 ● Trials 9–11 used a slightly different event definition where the calibration poses were not
436 explicitly tagged by an event, yet the protocol was identical to the following trials. The
437 calibration pose will have to be determined manually.

438 ● During trials 9–15, we used wooden blocks to fix the treadmill to the concrete floor to eliminate
439 the treadmill’s low vibration mode. But these blocks seem to have corrupted the force plate
440 measurements by imposing frictional stresses on the system. The force plate measurements
441 should not be used from these trials.

442 ● We did not record unloaded compensation trials for trials 9–15. Regardless, they would likely
443 be useless due to the corruption from the wooden blocks and are not needed because the
444 treadmill base is fixed.

445 CONCLUSION

446 We have presented a rich and elaborate data set of motion and ground reaction loads from human
447 subjects during both normal walking and when recovering from perturbations. The raw data is
448 provided for reuse with complete meta data. In addition to the data, we provide software that can
449 process the data for both cleaning purposes and to produce typical sagittal plane gait variables of
450 interest. Among other uses, we believe the dataset is ideally suited for control identification purposes.
451 Many researchers are working on mathematical models for control in gait and this dataset provides
452 both a way to validate these models and a source for generating them.

453 DATA AVAILABILITY

454 The data set (Moore et al., 2014a) is available via two Zenodo data repositories. The first holds
455 two approximately 1.2GB gzipped tar balls with contain the main data and a README file with a
456 short description of the contents. The second (Hnat et al., 2015) contains the Simulink generated
457 data for the treadmill control inputs. The data is released under the Creative Commons CC0 license
458 (<http://creativecommons.org/about/cc0>) following best practices for sharing scientific data.

459 SOFTWARE AVAILABILITY

460 The tables, figures, and the paper can be reproduced from the source repository shared on Github:
461 <https://github.com/csu-hmc/perturbed-data-paper>. Along with the source code in the repository, the
462 computations depend on version 0.1.2 of the GaitAnalysisToolKit (Moore et al., 2014b) which can
463 be downloaded from Zenodo or the Python Package Index (<http://pypi.python.org>).

464 AUTHOR CONTRIBUTIONS

465 A.v.d.B. conceived of the experiments and protocol. J.K.M and S.K.H refined the protocol, ran
466 the experiments, collected the data, developed the software, and analyzed the data. J.K.M was the
467 primary author of the paper with significant contributions from S.K.H and A.v.d.B. All authors were
468 involved in the revision of the draft manuscript and have agreed to the final content.

469 COMPETING INTERESTS

470 The authors have no financial, personal, or professional competing interests that could be construed
471 to unduly influence the content of this article.

472 GRANT INFORMATION

473 The work was partially funded by the State of Ohio Third Frontier Commission through the Wright
474 Center for Sensor Systems Engineering (WCSSE) and by the National Science Foundation under
475 Grant No. 1344954.

476 ACKNOWLEDGMENTS

477 We thank Roman Boychuk and Obinna Nwanna for assistance with the experiments. We also thank
478 Sabrina Abram, Brad Humphreys, and Anne Koelewijn for reviewing the preprint and being our

479 guinea pigs on the software/data instructions. Dan Simon also gave valuable feedback on the preprint.
480 Furthermore, we thank the academic editor, Arti Ahluwalia, and three reviewers, Morgan Sangeux,
481 Paul Lee, and Manoj Srinivasan, for their valuable feedback which helped improve the quality of the
482 paper and data.

483 REFERENCES

- 484 Chester, V. L., Tingley, M., and Bideen, E. N. (2007). Comparison of two normative paediatric gait
485 databases. *Dynamic Medicine*, 6(8).
- 486 European Commission (2012). Scientific data: Open access to research results will boost Europe's
487 innovation capacity.
- 488 Geyer, H. and Herr, H. (2010). A muscle-reflex model that encodes principles of legged mechanics
489 produces human walking dynamics and muscle activities. *Neural Systems and Rehabilitation
490 Engineering, IEEE Transactions on*, 18(3):263–273.
- 491 Hnat, S. and van den Bogert, A. J. (2014). Inertial compensation for belt acceleration in an
492 instrumented treadmill. *Journal of Biomechanics*, 47(15):3758–3761.
- 493 Hnat, S. K., Moore, J. K., and van den Bogert, A. J. (2015). Commanded Treadmill Motions for
494 Perturbation Experiments. <http://dx.doi.org/10.5281/zenodo.16064>.
- 495 Hodgins, J. (2015). CMU Graphics Lab Motion Capture Database. <http://mocap.cs.cmu.edu>.
- 496 Hunter, J. D. (2007). Matplotlib: A 2D graphics environment. *Computing In Science & Engineering*,
497 9(3):90–95.
- 498 Jones, E., Oliphant, T., Peterson, P., et al. (2001). SciPy: Open source scientific tools for Python.
- 499 Kirtley, C. (2014). CGA Normative Gait Database. <http://www.clinicalgaitanalysis.com/data/>.
- 500 Makihara, Y., Mannami, H., Tsuji, A., Hossain, M., Sugiura, K., Mori, A., and Yagi, Y. (2012). The
501 OU-ISIR gait database comprising the treadmill dataset. *IPSJ Trans. on Computer Vision and
502 Applications*, 4:53–62.
- 503 McKinney, W. (2010). Data structures for statistical computing in Python. In *Proceedings of the 9th
504 Python in Science Conference*, pages 51–56.
- 505 Moore, J. K., Hnat, S., and van den Bogert, A. (2014a). An elaborate data set on human gait and the
506 effect of mechanical perturbations. <http://dx.doi.org/10.5281/zenodo.13030>.
- 507 Moore, J. K., Nwanna, O., Hnat, S., and van den Bogert, A. (2014b). GaitAnalysisToolKit: Version
508 0.1.2. <http://dx.doi.org/10.5281/zenodo.13159>.
- 509 Octave community (2014). GNU Octave 3.8.1.
- 510 Sup, F., Bohara, A., and Goldfarb, M. (2008). Design and control of a powered transfemoral
511 prosthesis. *The International Journal of Robotics Research*, 27(2):263–273.
- 512 Tirosh, O., Baker, R., and McGinley, J. (2010). GaitaBase: Web-based repository system for gait
513 analysis. *Computers in Biology and Medicine*, 40(2):201–207.
- 514 van den Bogert, A. J. (2003). Exotendons for assistance of human locomotion. *BioMedical
515 Engineering OnLine*, 2(17).
- 516 van den Bogert, A. J., Geijtenbeek, T., Even-Zohar, O., Steenbrink, F., and Hardin, E. C. (2013). A
517 real-time system for biomechanical analysis of human movement and muscle function. *Medical
518 & Biological Engineering & Computing*, 51(10):1069–1077.
- 519 Vaughan, C., Davis, B., and O'Connor, J. (1992). *Dynamics of Human Gait*. Human Kinetics
520 Publishers, 1st edition.
- 521 Walt, S. v. d., Colbert, S. C., and Varoquaux, G. (2011). The NumPy Array: A structure for efficient

- 522 numerical computation. *Computing in Science & Engineering*, 13(2):22–30.
- 523 Wang, Y. and Srinivasan, M. (2014). Stepping in the direction of the fall: The next foot place-
524 ment can be predicted from current upper body state in steady-state walking. *Biology Letters*,
525 10(9):20140405.
- 526 White, E. P., Baldrige, E., Brym, Z. T., Locey, K. J., McGlinn, D. J., and Supp, S. R. (2013). Nine
527 simple ways to make it easier to (re)use your data. *PeerJ PrePrints*, 1:e7v2.
- 528 White House (2013). Increasing access to the results of federally funded scientific research.
- 529 Willson, J. D. and Kernozek, T. (2014). Gait data collected at University of Wisconsin-LaCrosse.
530 <http://www.innsport.com/related-products/data-sets/uw-l-gait-data-set.aspx>.
- 531 Winter, A., D. (1990). *Biomechanics and Motor Control of Human Movement*. John Wiley and
532 Sons, Inc, 2nd edition.
- 533 Yun, Y., Kim, H.-C., Shin, S. Y., Lee, J., Deshpande, A. D., and Kim, C. (2014). Statistical method
534 for prediction of gait kinematics with Gaussian process regression. *Journal of Biomechanics*,
535 47(1):186–192.

```

study:
  id: 1
  name: Gait Control Identification
  description: Perturb the subject during walking and running.
subject:
  id: 8
  age: 20
  mass: 70.0
  mass-units: kilograms
  height: 1.572
  height-units: meters
  knee-width-left: 107.43
  knee-width-right: 107.41
  knee-width-units: millimeters
  ankle-width-left: 70.52
  ankle-width-right: 67.66
  ankle-width-units: millimeters
  gender: male
trial:
  id: 58
  subject-id: 8
  datetime: 2014-03-28
  notes: >
    The subject did a somersault during this trial instead of following
    instructions to walk. Will have to use for another study.
  nominal-speed: 0.8
  nominal-speed-units: meters per second
  stationary-platform: True
  pitch: False
  sway: False
  hardware-settings:
    high-performance: True
  dflow-version: 3.16.1
  cortex-version: 3.1.1.1290
  marker-set: full
  marker-map:
    M1: LHEAD
    M2: THEAD
    M3: RHEAD
    M4: FHEAD
    M5: C7
  analog-channel-map:
    Channel1.Anlg: F1Y1
    Channel2.Anlg: F1Y2
    Channel3.Anlg: F1Y3
    Channel4.Anlg: F1X1
  events:
    A: Force Plate Zeroing
    B: Calibration Pose
    C: First Normal Walking
    D: Longitudinal Perturbation
    E: Second Normal Walking
    F: Unloaded End
  files:
    compensation: ../T057/mocap-057.txt
    mocap: mocap-058.txt
    record: record-058.txt
    meta: meta-058.yml

```

Listing 1. A fictitious example of a YAML formatted meta data file. Examples of all of the possible keys in the data set are shown.

```
>>> from gaitanalysis.motek import DFlowData
>>> data = DFlowData('mocap-020.txt', 'record-020.txt',
...                  'meta-020.yml')
>>> mass = data.meta['subject']['mass']
>>> data.clean_data()
>>> event_df = data.extract_processed_data(
...     event='Longitudinal Perturbation')
```

Listing 2. Python interpreter session showing how one could load a trial into memory, extract the subject's mass from the meta data, run the data cleaning process, and finally extract a Pandas DataFrame containing all of the time histories for a specific event in the trial.

```
>>> from gaitanalysis.gait import GaitData
>>> gdata = GaitData(event_df)
>>> gdata.inverse_dynamics_2d(left_markers, right_markers,
...                           left_loads, right_loads, mass, 6.0)
>>> gdata.grf_landmarks('Right Fy', 'Left Fy', threshold=20.0)
>>> gdata.split_at('right')
>>> gdata.plot_gait_cycles('Left Hip Joint Torque', mean=True)
>>> gdata.save('gait-data.h5')
```

Listing 3. Python interpreter session showing how one could use the GaitData class to load in the result of DFlowData and compute the inverse dynamics (joint angles and torques), identify the gait events (e.g. heel strikes), split the data with respect to the gait events into a Pandas Panel, plot the mean and standard deviation of one time history with respect to the gait cycles, and save the data to disk.